

## Design and realization of InP-based resonant tunneling diode THz oscillator

LIU Jun<sup>1\*</sup>, SONG Rui-Liang<sup>1</sup>, LIU Ning<sup>1</sup>, LIANG Shi-Xiong<sup>2</sup>

1. 54th Research Institute, China Electronics Technology Group Corporation (CETC54), Beijing 100070, China;
2. The National Key Laboratory of ASIC, Hebei Semiconductor Research Institute, Shijiazhuang 050051, China)

**Abstract:** An oscillator above 1 THz is designed and realized using InP-based resonant tunneling diode (RTD) and an on-chip antenna with Si-lens. The RTD model was built and studied with Silvaco software. The influences of the doping concentration of emitter, the thickness of barrier layer, space layer, and well layer on the DC characteristics of the device have been analyzed. The DC measurement of the RTD shows the peak current density  $J_p = 359.2 \text{ kA/cm}^2$ , the valley current density  $J_v = 135.8 \text{ kA/cm}^2$ , and the peak-to-valley current ratio (PVCRR) = 2.64. According to the measurement, the maximum RF output power and oscillation frequency ( $f_{\max}$ ) are theoretically calculated, which are 1.71 mW and 1.49 THz, respectively. The oscillator with an on-chip bow-tie antenna and RTD is packaged with Si-lens. The measurement shows the output power is 2.57  $\mu\text{W}$  at an operation frequency of above 1 THz, the DC power consumption is 8.33 mW. This is the first reported oscillator of frequency above 1 THz in domestic.

**Key words:** THz, resonant tunneling diode, oscillator

**PACS:** 07. 57. Kp

## InP 基共振隧穿二极管太赫兹振荡器的设计与实现

刘 军<sup>1\*</sup>, 宋瑞良<sup>1</sup>, 刘 宁<sup>1</sup>, 梁士雄<sup>2</sup>

1. 中国电子科技集团公司第五十四研究所北京研发中心, 北京 100070;
2. 河北半导体技术研究所专用集成电路国家重点实验室, 河北 石家庄 050051)

**摘要:** 利用 InP 基共振隧穿二极管 (RTD) 和加载硅透镜的片上天线设计实现了超过 1 THz 的振荡器。采用 Silvaco 软件对 RTD 模型进行仿真研究, 分析了不同发射区掺杂浓度、势垒层厚度、隔离层厚度以及势阱层厚度等对器件直流特性的影响规律。对研制的 RTD 器件直流特性测试显示: 峰值电流密度  $J_p$  为  $359.2 \text{ kA/cm}^2$ , 谷值电流密度  $J_v$  为  $135.8 \text{ kA/cm}^2$ , 峰谷电流比 PVCRR 为 2.64, 理论计算得到的器件最大射频输出功率和振荡频率 ( $f_{\max}$ ) 分别为 1.71 mW 和 1.49 THz。利用透镜封装的形式对采用 Bow-tie 片上天线和 RTD 设计的太赫兹振荡器进行封装, 测试得到振荡频率超过 1 THz, 输出功率为 2.57  $\mu\text{W}$ , 直流功耗为 8.33 mW, 是国内首次报道超过 1 THz 的振荡器。

**关键词:** 太赫兹; 共振隧穿二极管; 振荡器

中图分类号: O43 文献标识码: A

### Introduction

The terahertz (THz) frequency band (0.3~10 THz) has attracted fast-growing research interests due to its many possible applications, such as imaging systems for radar or security imaging, spectroscopy in chemistry and biotechnology and high-data-rate communications<sup>[1-6]</sup>.

The compact and coherent solid-state THz signal sources are considered to be the key components for these applications. Compared with any other traditional electronic devices such as field-effect or bipolar transistors (MOS-FETs, HEMTs or HBTs), or diode technologies (IMPATT, Gunn, etc.), the resonant tunneling diodes (RTDs) have also been considered as one of the most

**Received date:** 2021-04-25, **revised date:** 2022-01-17

**收稿日期:** 2021-04-25, **修回日期:** 2022-01-17

**Foundation items:** Supported by National Key R&D Program of China (2018YFE0202500), National Key Research and Development Program of China (2017YFC08219), Manned Space Advanced Research Project (060401), Advanced Research Project of Civil Aerospace Technology (B0105).

**Biography:** LIU Jun (1989-), male, Shandong, China, Engineer, Ph. D. Research area involves terahertz device, circuit and package for imaging. E-mail: lj\_bit@163.com

\* **Corresponding author:** E-mail: lj\_bit@163.com

promising candidates for THz oscillators at room temperature<sup>[7-10]</sup>. The advantages of RTDs include the facts that they can exhibit the highest oscillation frequency of the inherent negative differential conductance (NDC) due to the resonant tunneling among the electronic devices and consume low power, as well as the output power is easily modulated through the bias network and can operate at room temperature.

In this paper, we propose and fabricate a THz oscillator with InP-based RTD and dielectric lens antenna. The influences of material structure including the doping concentration of emitter, the thickness of barrier layer, space layer, and well layer on the DC characteristics are analyzed by Silvaco software. Excellent DC characteristics of the RTD are demonstrated with  $J_p = 359.2 \text{ kA/cm}^2$ ,  $J_v = 135.8 \text{ kA/cm}^2$ , and  $\text{PVCr} = 2.64$ . The oscillator is packaged with Si-lens and exhibits the output power of  $2.57 \mu\text{W}$  at an operation frequency above 1 THz.

## 1 RTD device

RTDs are commonly realized in GaAs and InP. Compared with GaAs, InP material system offers better properties in the conduction band offset, the electron effective mass.  $\text{In}_{0.53}\text{Ga}_{0.47}\text{As}$  can also be highly doped when used as the RTD device electrodes to reduce the Ohmic contact resistance. The material system for the RTD device utilized in this project is InGaAs/AlAs. InP-based RTD device is typically consisted of a narrow bandgap material (4~6 nm thick quantum well) sandwiched between two thin wide bandgap materials (1~3 nm AlAs barriers), making up a double barrier quantum well (DBQW) structure. The structure is completed by lightly doped InGaAs spacer layers, n-type emitter/collector layers, and highly doped InGaAs contact layers on each side of the DBQW, as shown in Fig. 1.

The 2D structure of the device is defined in Deck-build based on the material structure as shown in Fig. 1 by using the Atlas, which a device simulation product originating simulated from Silvaco. The relationship between the epi-layer structure and DC characteristics has been researched on the doping concentration of emitter, the thickness of barrier layer ( $t_b$ ), well layer ( $t_w$ ) and spacer layer ( $t_s$ ). In order to observe the relationship between the material structure and DC characteristics more intuitively, the peak current ( $I_p$ ) and peak voltage ( $V_p$ ) of the device are mainly analyzed, as shown in Fig. 2. The simulation results in Fig. 2 shows that the performance of RTD devices is closely related to the epitaxial material structure. In order to realize a high-power, high-frequency RTD device, the electrical characteristics of the device is optimized mainly by optimizing the negative

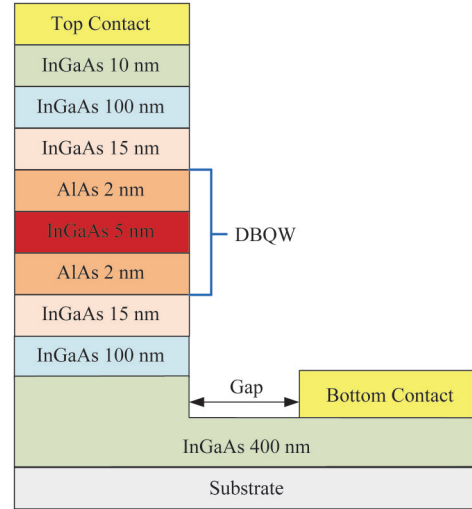


Fig. 1 Illustration of InP-based RTD structure  
图1 InP基RTD结构示意图

differential conductance region (NDR) in the I-V curve in this design. After optimization, the RTD material structure designed in this study is shown in Table 1.

The RTD epi-material is grown on a 3-inch wafer using molecular beam epitaxy (MBE). The photograph of the manufactured InP-based RTD device with an emitter area of  $12 \mu\text{m}^2$  is shown in Fig. 3 (a). Characterization of the device was done by on-wafer measurements with B1500A Semiconductor Device Parameter Analyzer at room temperature. The on-wafer measured I-V characteristic of the RTD device is depicted in Fig. 3 (b). The RTD shows peak voltage  $V_p=0.91 \text{ V}$ , peak current  $I_p=43.1 \text{ mA}$ , peak current density  $J_p=I_p/A=359.2 \text{ kA/cm}^2$ , and peak-to-valley current ratio  $\text{PVCr}=I_p/I_v=2.64$ .

Figure 4 shows the small-signal equivalent circuit of the RTD. The total series resistance ( $R_s$ ) of the diode includes ohmic contact resistance, spreading resistance, and resistance due to the epitaxial layer. The  $R_s \approx 4.8 \Omega$  is estimated from transmission line measurements (TLM). The self-capacitance ( $C_n$ ) represents the charging and discharging effect of electrons at the semiconductor depletion regions. The  $C_n \approx 11 \text{ fF}$  is measured by B1500A. The quantum-well inductance ( $L_{qw}$ ) represents the electron dwell time in quantum well and will not limit the oscillator frequency<sup>[11]</sup>.

The frequency dependent impedance of the RTD is given by Eq. 1.

$$Z(f) = R(f) + jX(f) \quad (1)$$

The maximum oscillation frequency ( $f_{\text{max}}$ ) of the RTD is defined as the frequency where  $R(f)$  becomes zero, as given by Eq. 2.

$$f_{\text{max}} = \frac{1}{2\pi} \sqrt{\frac{1}{2L_{\text{qw}}^2 C_n}} \left\{ 2L_{\text{qw}} - \frac{C_n}{C_n^2} + \sqrt{\left[ \left( \frac{C_n}{C_n^2} - 2L_{\text{qw}} \right)^2 - \frac{4 - L_{\text{qw}}(1 + R_s G_n)}{R_s G_n} \right]} \right\} \quad (2)$$

Equation 2 simplifies to Eq. 3 when  $L_{\text{qw}}$  is assumed to be negligibly small.

$$f_{\text{max}} = \frac{1}{2\pi C_n} \sqrt{\frac{G_n}{R_s} - G_n^2} \quad (3)$$

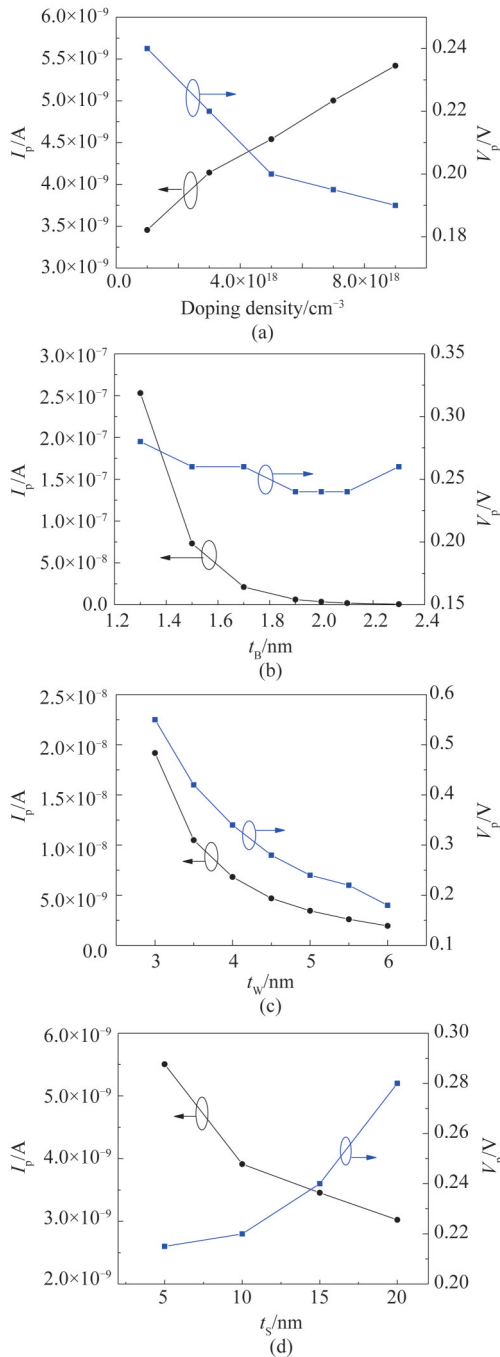


Fig. 2 Peak voltage ( $V_p$ ) and peak current ( $I_p$ ) vs (a) doping density, (b)  $t_b$ , (c)  $t_w$ , (d)  $t_s$   
图2 峰值电压和峰值电流随(a)掺杂浓度, (b)势垒层厚度  $t_b$ , (c)势阱层厚度  $t_w$ , (d)隔离层厚度  $t_s$ 的变化

The RTD negative conductance ( $G_n$ ) is given by

$$G_n = \frac{3\Delta I}{2\Delta V} \quad (4)$$

where  $\Delta I = I_p - I_v$ ,  $\Delta V = V_p - V_v$ .

The maximum available RF output power ( $P_{\max}$ ) that a RTD-based oscillator can deliver to the load, which is given by

$$P_{\max} = \frac{3}{16} \Delta V \Delta I \quad (5)$$

Table 1 The layer structure of the RTD device used in this study

表1 采用的RTD外延层结构

Composition	Doping/ $\text{cm}^{-3}$	Thickness/nm
$n^+$ -In <sub>0.7</sub> Ga <sub>0.3</sub> As	$2 \times 10^{19}$	8
$n^+$ -In <sub>0.53</sub> Ga <sub>0.47</sub> As	$2 \times 10^{19}$	15
$n^+$ -In <sub>0.53</sub> Ga <sub>0.47</sub> As	$3 \times 10^{18}$	25
un-In <sub>0.53</sub> Ga <sub>0.47</sub> As		20
un-AlAs		1.2
un-In <sub>0.8</sub> Ga <sub>0.2</sub> As		5
un-AlAs		1.2
un-In <sub>0.53</sub> Ga <sub>0.47</sub> As		2
$n^+$ -In <sub>0.53</sub> Ga <sub>0.47</sub> As	$3 \times 10^{18}$	20
$n^+$ -In <sub>0.53</sub> Ga <sub>0.47</sub> As	$2 \times 10^{19}$	400
un-In <sub>0.53</sub> Ga <sub>0.47</sub> As		200
InP Substrate		

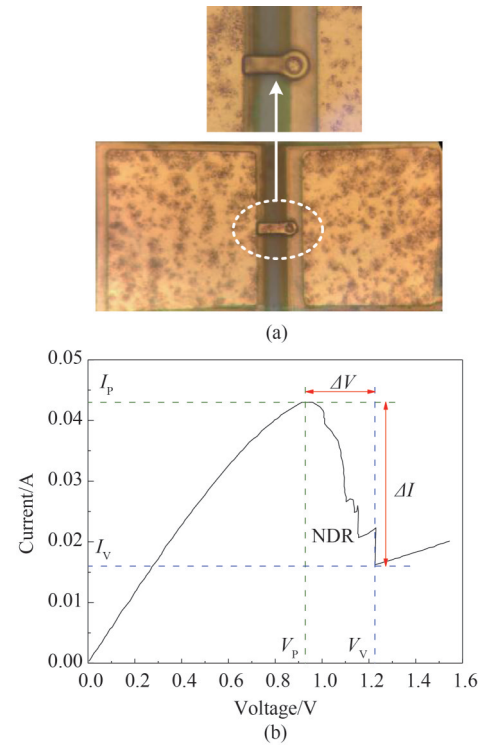


Fig. 3 (a) Photo of the fabricated RTD, (b) measured  $I$ - $V$  characteristic of the RTD device  
图3 (a)研制的RTD器件照片, (b)器件  $I$ - $V$ 测试曲线

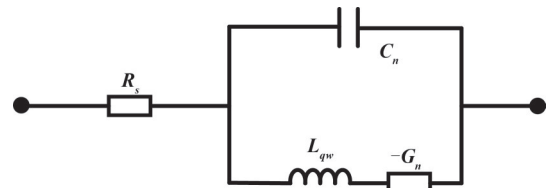


Fig. 4 Small-signal equivalent circuit of RTD  
图4 RTD小信号等效电路模型

According to Eqs. 3-5, the theoretical  $f_{\max}$  of the RTD is evaluated to be 1.49 THz and the theoretical  $P_{\max}$

=1.71 mW. The DC measurement results of the RTD device and theoretical oscillation frequency and maximum RF output power are summarized in Table 2.

**Table 2** RTD DC parameter and theoretical oscillation frequency and maximum RF output power

表 2 RTD 直流参数和理论振荡频率以及最大射频输出功率

$I_p$ /mA	$I_v$ /mA	$V_p$ /V	$V_v$ /V	PVCR	$J_p$ (kA/cm <sup>2</sup> )	$J_v$ (kA/cm <sup>2</sup> )	$f_{max}$ /THz	$P_{max}$ /mW
43.1	16.3	0.91	1.26	2.64	359.2	135.8	1.49	1.71

### 3 Bow-tie antenna

Bow-tie antenna is a widely used wideband antenna in terahertz band. The proposed bow-tie shape THz antenna is shown in Fig. 5 (a) and patterned over 25 μm InP substrate. Due to the lower gain of the proposed antenna, a silicon lens is mounted over the antenna as depicted in Fig. 5 (b). The simulation of the proposed antenna is carried out in CST Microwave Studio. Fig. 6 shows the variation of the Voltage Standing Wave Ratio (VSWR) and gain of the proposed antenna with Si-lens which indicates more than 200 GHz impedance bandwidth spanning from 0.9 to 1.1 THz and 13.7 dBi gain.

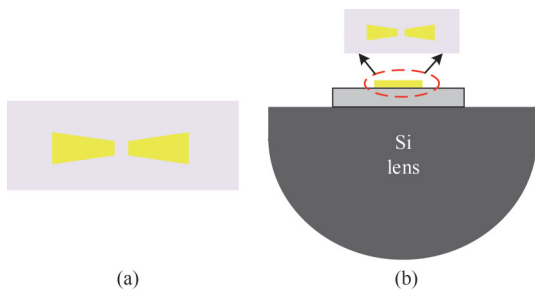


Fig. 5 (a) schematic of the proposed bow-tie antenna, (b) antenna with Si-lens mounting  
图5 (a) 本文采用的 Bow-tie 天线结构, (b) 加载硅透镜后天线结构示意图

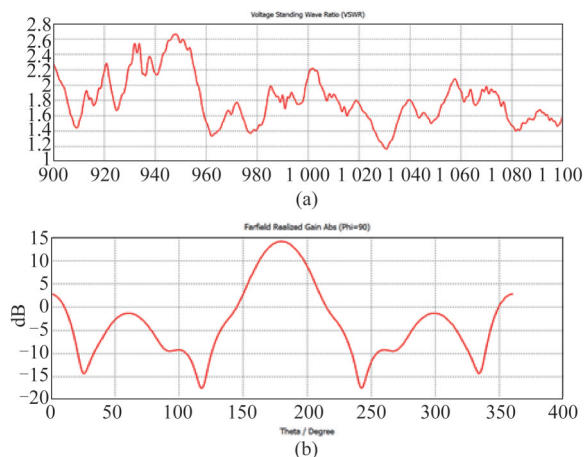


Fig. 6 (a) VSWR and (b) gain of the proposed antenna with Si-lens  
图6 加载硅透镜天线的(a)驻波比和(b)增益

### 4 Oscillator measurement

Figure 7 presents the package configuration of the quasi-optical RTD oscillator. It consists of RTD oscillator by integrating RTD with a bow-tie antenna, a highly resistive Si-lens and a low-frequency PCB. The fabricated chip is mounted on Si-lens and wire-bonded with Au wires with a diameter of 50 μm onto PCB for the measurements of the oscillation characteristics.

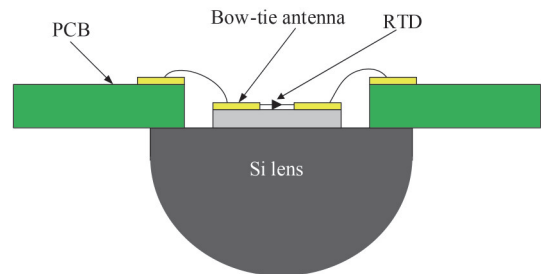


Fig. 7 Schematic of oscillator package  
图7 振荡器封装示意图

Figure 8 shows the RTD oscillator packaged with PCB and the detail of RTD oscillator. The THz signal is generated from the RTD oscillator and radiate into air through Si-lens.

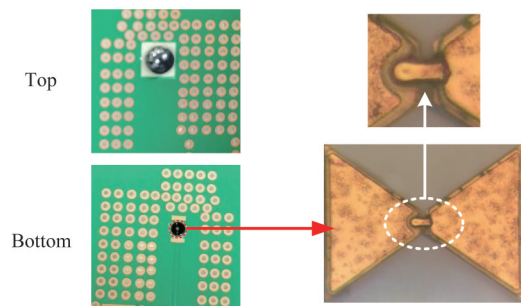


Fig. 8 The photograph of the packaged oscillator  
图8 振荡器封装实物图

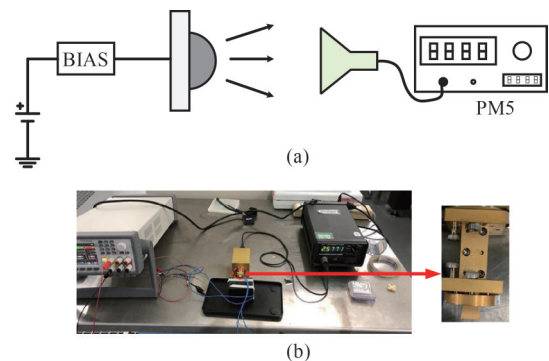


Fig. 9 (a) Block diagram of measurement scheme, (b) photo of the test environment  
图9 (a)测试方案框图, (b)实际测试环境

In order to characterize the performances of the fabricated oscillator, the room temperature measurement is

performed and the block diagram of the measurement scheme is shown in Fig. 9 (a). Due to lacking 1 THz spectrum analyzer, 0.75~1.1 THz horn antenna and WR0.65 (1.1~1.7 THz) convert waveguide are used with PM5 for measuring the output power and frequency as shown in Fig. 9 (b). The best performances of the fabricated oscillator are obtained at an applied bias voltage of 0.95 V with a current of 8.7 mA. A peak output power of 2.57  $\mu\text{W}$  is obtained above 1 THz. The DC power consumption of the RTD oscillator is 8.33 mW, while the DC-to-RF power efficiency is 0.0308% at the operation frequency.

## Conclusion

A THz RTD oscillator is designed and fabricated based on InP RTD MMIC technology. The RTD device shows theoretically calculated maximum RF output power of 1.71 mW and  $f_{\text{max}}$  of 1.49 THz. The oscillator shows an output power of 2.57  $\mu\text{W}$  with a DC power consumption of 8.33 mW above 1 THz. This work shows the potential of the RTD oscillator topology as a practical THz signal source for future THz applications. To our knowledge, this is the first reported oscillator of frequency above 1 THz in domestic.

## References

- [1] LIU Jun, HE Wei, QIAO Hai-Dong, *et al.* The study and application of D-band radiometer front-end[J]. *Journal of Infrared Millimeter Waves*(刘军,何伟,乔海东,等。D波段辐射计前端的设计与应用。《红外与毫米波学报》),2020,39(6):704-708.
- [2] WU Ju-Xiu, YANG Lei, DOU Fang-Li, *et al.* The detection capability to ice clouds for space-borne terahertz dual-frequency radar [J].*Journal of Infrared Millimeter Waves*(吴举秀,杨蕾,窦芳丽,等。星载太赫兹双频云雷达对冰云探测能力研究。《红外与毫米波学报》),2020,39(6):718-727.
- [3] CHEN Jing-Yuan, LIN Zhong-Xi, LIN Qi, *et al.* Design and simulation of dual-frequency terahertz antenna for wireless communication by photo mixing[J]. *Journal of Infrared Millimeter Waves*(陈京源,林中晞,林琦,等。基于光混频的太赫兹双频通信天线的设计和仿真。《红外与毫米波学报》),2019,38(4):493-498.
- [4] YANG Yi-Lin, ZHANG Bo, JI Dong-Feng, WANG Yi-Wei, ZHAO Xiang-Yang, FAN Yong. A wideband terahertz planar Schottky diode fourth-harmonic mixer with low LO power requirement [J]. *Journal of Infrared Millimeter Waves*(杨益林,张波,纪东峰,等。基于肖特基二极管的宽带低本振功率太赫兹四次谐波混频器。《红外与毫米波学报》),2020,39(5):540-546.
- [5] Dan I, Szriftgiser P, Peytavit E, *et al.* 300 GHz wireless link employing a photonic transmitter and active electronic receiver with a transmission bandwidth of 54 GHz [J]. *IEEE Transactions on Terahertz Science and Technology*, 2020, 99:1-1.
- [6] LIU Song-Zhuo, YU Wei-Hua, DENG Chang-Jiang, *et al.* Recent progress of research on terahertz signal modulation technology for communication systems [J]. *Radio Communications Technology*(刘松卓,于伟华,邓长江,等。面向通信系统的太赫兹调制技术进展现状。《无线电通信技术》),2021,47(1):44-50.
- [7] Suzuki S, Asada M, Teranishi A, *et al.* Fundamental oscillation of resonant tunneling diodes above 1 THz at room temperature[J]. *Applied Physics Letters*, 2010, 97(24):97.
- [8] Feiginov M, Kanaya H, Suzuki S, *et al.* 1.46 THz RTD oscillators with strong back injection from collector[C]. 2014 39th International Conference on Infrared, Millimeter, and Terahertz waves (IRMMW-THz), Tucson, AZ, USA, 2014, pp. 1-2, doi: 10.1109/IRMMW-THz.2014.6956452.
- [9] Asada M, Maekawa T, Kanaya H, *et al.* Frequency increase in terahertz oscillation of resonant tunnelling diode up to 1.55 THz by reduced slot-antenna length[J]. *Electronics Letters*, 2014, 50(17):1214-1216.
- [10] Izumi R, Suzuki S, Asada M. 1.98 THz resonant-tunneling-diode oscillator with reduced conduction loss by thick antenna electrode [C]. IEEE, 2017:1-2.
- [11] Wang J, Al-Khalidi A, Cornescu A, *et al.* Design, fabrication and characterisation of RTD terahertz oscillators[C]. 2019 European Microwave Conference in Central Europe (EuMCE), Prague, Czech Republic, 2019, pp. 261-264.